Sustainable Materials and Technologies 31 (2022) e00369

Contents lists available at ScienceDirect

Sustainable Materials and Technologies

journal homepage: www.elsevier.com/locate/susmat

Impact of the lignin type and source on the characteristics of physical lignin hydrogels

Amaia Morales [a], Jalel Labidi [a,*], Patricia Gullón [b]

[a] Chemical and Environmental Engineering Department, University of the Basque Country UPV/EHU, Plaza Europa 1, 20018 San Sebastián, Spain
[b] Centro de Apoio Científico e Tecnolóxico á Investigación, Universidade de Vigo, Technology Park of Galicia- Tecnopole, CTC Building, 32901, San Cibrao das Viñas, Ourense, Spain

ARTICLE INFO

Keywords:
Lignin
Poly (vinyl alcohol)
Almond shells
Walnut shells
Physical hydrogels

ABSTRACT

Multiple natural polymers have been investigated for the synthesis of hydrogels to the present date, but lignin has demonstrated to be a promising one for this purpose for the multiple advantages it offers. Lignin can be isolated from lignocellulosic material such as nut shells, which are usually undervalued wastes, and would be a great step forward on circular economy. Thus, in the present work, lignin was extracted from almond and walnut shells following a single-step (delignification) and double-step (autohydrolysis and delignification) biorefinery scheme. After the chemical composition and structures of these lignins were determined, hydrogels were synthesized combining them with poly (vinyl alcohol) by the means of freeze-thawing cycles so as to study the influence of the different lignins on their final properties. Additionally, the last thawing cycle of the synthesis process was lengthened in order to confirm previous assumptions about its effect on the characteristics of the synthesized materials. The obtained results showed significant variation between the 8 lignin samples, especially in their purity, molecular weights and total phenolic contents. The variation on the lignins leaded to several hydrogel morphologies, which directly affected their properties, primarily their swelling capacity, glass transition temperatures and compression strengths. It was also demonstrated the great effect that the duration of the last thawing had on the morphology and, hence, on the characteristics of the obtained materials. The synthesized samples were successfully employed as dye adsorbents and the evaluation of their antifungal activity showed positive results in some of the samples, which could be applied for food packaging.

1. Introduction

Synthetic polymer-based items like hydrogels have completely stirred up our everyday lives. These materials are comprised by tridimensionally entangled polymeric chains that exhibit high water retention capacity due to the multiple hydrophilic groups they contain [1]. In addition to their great swelling properties, their internal structure together with their mechanical properties have made them gain considerable attention in the last years [2]. Hydrogels can be arranged according to the types of crosslinks that their polymeric chains present, which can be physical or chemical [2]. The chemical ones often demand the presence of toxic and costly crosslinking reagents whereas the physical ones do not. Thus, physical crosslinking makes the synthesis process greener and more economical [3]. Hydrogels can be presented in many substrates and forms, which, together with the aforementioned features, make them useful in a wide range of applications such as agriculture and environment, personal hygiene or biomedicine, among others [1].

The beginning of the 21st century has been marked by a significant economic boost coupled with high plastic pollution which have leaded to several irrecoverable environmental concerns. In this context, the possibility of introducing biodegradable and renewable polymers to produce new materials such as hydrogels is nowadays one of the principal goals of research. Biopolymers, which are polymers coming from plants, animals and microorganisms, seem to be the solution to the stated problem since, apart from helping to face ecological problems [4], they would also contribute to sustainability and circular economy [5].

Biopolymers and other co-products (e.g. biofuels and biochemicals) can be extracted from biomass through biorefinery processes [6]. Lignocellulosic biomass, for instance, has emerged as a potential, renewable and available source of biopolymers and biochemicals. This type of biomass involves forestry, urban and alimentary residues [7].

* Corresponding author.
E-mail address: jalel.labidi@ehu.eus (J. Labidi).

https://doi.org/10.1016/j.susmat.2021.e00369
Received 5 July 2021; Received in revised form 14 September 2021; Accepted 26 November 2021
Available online 29 November 2021

The main constituents of lignocellulosic biomass are cellulose, hemicelluloses and lignin, which can be employed as backbones on the formulation of hydrogels and other materials.

Among these natural polymers, lignin is the most bountiful aromatic one on Earth [8]. Its amorphous and complex structure is principally constituted by a random combination of three kinds of phenyl propane monomers (coniferyl, *p*-coumaryl and sinapyl alcohols) connected through several stable linkages [8]. The isolation method influences the properties of the extracted lignin such as its reactivity. The typical lignin extraction methods include Kraft, sulphite, alkaline and organosolv delignifications [9]. Lignin is commonly obtained as a by-product of pulp and paper industries; nevertheless, a small percentage of the entire quantity (<2%) of lignin generated every year has an added-value [8]. Hence, employing it for the synthesis of hydrogels, for instance, would contribute to cover the urgent need of safe and greener alternative materials.

Almond and walnut shells are an abundant waste all over the world. The low percentage of edible kernel in both nuts leads to an enormous production of shells with no recognized industrial or commercial application [7,10]. However, these shells belong to the lignocellulosic biomass and are very rich in lignin and other biopolymers. Therefore, these residues could be further valorised though a biorefinery strategy so as to use them as input feedstocks for the production of added-value materials [7,10].

In the last years, several researchers have described the synthesis of hydrogels with lignin from different sources and with different extraction methods [11,12]. Nonetheless, a great part of the published works reports the production of chemically crosslinked hydrogels, generally involving the use of toxic crosslinkers as well as the need of removing the residual part of it [3].

In this light, the objective of the present study was to analyse the influence of the type of lignin and its features on the final characteristics of physically crosslinked lignin-hydrogels. For this aim, lignin was extracted through alkaline and organosolv delignifications from walnut and almond shells (with and without prior hydrothermal pretreatment) [7,10] and hydrogels were formulated combining lignin and poly (vinyl alcohol) following the synthesis route reported previously [13]. In addition, hydrogels were also synthesized through a variation of the initial synthesis route, which consisted in lengthening the last thawing stage. In this way, the properties of these hydrogels were compared to the other ones, highlighting the most significant differences. The isolated lignins were characterised via purity, Py-GC/MS, HPSEC, FTIR, XRD, TGA and TPC analysis. The lignin waste and swelling capacity of all the synthesized hydrogels were measured and they were further characterised by FTIR, SEM, DSC and compression tests. Finally, the adsorption capacity of the hydrogels was evaluated by employing methylene blue as water pollutant, and their antifungal capacity against *Aspergillus niger* was also studied so as to explore their applicability in food packaging, for example.

2. Materials and methods

2.1. Materials

Almond shells (AS) were supplied by local farmers (Marcona variety) and walnut shells (WNS) were kindly supplied by Olagi cider house (Altzaga, Gipuzkoa). The shells were milled and sieved (particle size between 2 and 1 mm) and stored in a dark and dry place at room temperature until use.

Poly (vinyl alcohol) (M_w = 83,000–124,000 g/mol, 99 + % hydrolyzed), phosphate buffer saline (PBS) tablets, trypan blue solution and methylene blue powder were purchased from Sigma Aldrich. Sodium hydroxide (NaOH, analysis grade, ≥98%, pellets) was supplied by PanReac Química SLU. Potato dextrose agar (PDA) was acquired from Scharlab S.L. and DMSO from Fisher Scientific S.L. All reagents were employed as supplied.

2.2. Lignin extraction

The operational conditions were chosen in accordance to prior knowledge [7,10]. The alkaline and organosolv delignification stages were carried out twice for each type of shells: the first one without a prior hydrothermal treatment and the second one with a prior hydrothermal treatment (autohydrolysis). Table 1 summarizes the conditions employed for each lignin extraction.

2.3. Hydrogel synthesis

Lignin-hydrogels were synthesized according to a previous work [13]. The concentrations of the blends (9.87 w.% PVA and 9.12 w.% lignin) were also determined on the basis of previous studies. Briefly, the corresponding amount of PVA (5.92 g) was added to 60 mL of a 2% (*w*/w) NaOH aqueous solution and it was magnetically stirred and heated to 90 °C. Once the PVA was dissolved, lignin (5.47 g) was added while stirring until completel dissolution. The blends were poured into silicon moulds. The internal bubbles were eliminated by ultrasounds and the remaining superficial air bubbles were then poked manually.

The blends were frozen for 2.5 h at −20 °C and they were then thawed at 28 °C for 1.5 h. This cycle was repeated five times, leaving the samples freezing overnight during the second and fifth cycles. Afterwards, the hydrogels were washed as it was done previously [13] in order to remove the residual lignin and NaOH. Finally, the hydrogels were dried at room temperature.

Based on prior experiments (data not shown), it was thought that the duration of the last thawing step could alter the features of the synthesized hydrogels. For this reason, hydrogels with a longer 5th thawing stage (24 h inside the heater) were also prepared. These samples were tagged as LC samples (long cycle) and the previous ones as SC (short cycle).

2.4. Characterization methods

The characterization methods and equipments used in this work both for the extracted lignins and the synthesized hydrogels are described in Table 2.

2.5. Methylene blue adsorption tests

The removal of methylene blue (MB) was investigated according to a

Table 1
Operational conditions for each of the extracted lignins.

Abbreviation	Description	Autohydrolysis	Delignification
AAL	AS alkaline lignin	–	121 °C, 90 min, 7.5 w.% NaOH, LSR 6:1
AOL	AS organosolv lignin	–	200 °C, 90 min, 70/30 (*v*/*v*) EtOH/H_2O, LSR 6:1
WAL	WNS alkaline lignin	–	121 °C, 90 min, 7.5 w.% NaOH, LSR 6:1
WOL	WNS organosolv lignin	–	200 °C, 90 min, 70/30 (*v*/*v*) EtOH/H_2O, LSR 6:1
AAAL	Autohydrolysed AS alkaline lignin	179 °C (isothermal), 23 min, LSR 8:1	121 °C, 90 min, 7.5 w.% NaOH, LSR 6:1
AAOL	Autohydrolysed AS organosolv lignin	179 °C (isothermal), 23 min, LSR 8:1	200 °C, 90 min, 70/30 (*v*/*v*) EtOH/H_2O, LSR 6:1
AWAL	Autohydrolysed WNS alkaline lignin	200 °C (non-isothermal), LSR 8:1	121 °C, 90 min, 7.5 w.% NaOH, LSR 6:1
AWOL	Autohydrolysed WNS organosolv lignin	200 °C (non-isothermal), LSR 8:1	200 °C, 90 min, 70/30 (*v*/*v*) EtOH/H_2O, LSR 6:1

Table 2
Characterization methods and equipments for the extracted lignins and synthesized hydrogels.

Analysis	Sample	Equipment	Reference
Purity	Lignin	HPLC-RI/PDA (Jasco LC-Net II/ADC, 300 × 7.8 mm Aminex HPX-87H column)	[21]
Acid soluble lignin	Lignin	UV–Vis spectrophotometer (Jasco V-630, JASCO)	[18]
Composition	Lignin	Py-GC/MS (Py: 5150 Pyroprobe, GC: Agilent 6890, MS: Agilent 5973)	[21]
Average molecular weight	Lignin	GPC (JASCO LC-Netll/ADC, detector: RI-2031Plus,Two Polar Gel-M columns: 300 mm × 7.5 mm)	[18]
Total phenolic content (TPC)	Lignin	UV–Vis spectrophotometer (Jasco V-630, JASCO)	[18]
Thermal degradation	Lignin	TGA/DTG (TGA/SDTA RSI analyser 851 Mettler Toledo)	[13]
Crystallinity	Lignin	XRD (Phillips X'Pert Pro Automatic multipurpose diffractometer)	[13]
Chemical structure	Lignin	ATR-FTIR (PerkinElmer Spectrum Two FTIR Spectrometer)	[22]
Lignin Waste	Hydrogels	UV–Vis spectrophotometer (Jasco V-630, JASCO)	[13]
Swelling	Hydrogels	$Swelling\ (\%) = \frac{m_{swollen} - m_{dry}}{m_{dry}} x\ 100$	[13]
Morphology	Hydrogels	SEM (Hitachi S-4800, 5 kV, 20 nm Au covering)	[56]
Glass transition temperature	Hydrogels	DSC (Mettler Toledo DSC 822)	[13]
Compression tests	Hydrogels	Mechanical test machine (Instron 5967, 500 N load cell)	[13]

previous study [13]. In brief, first, multiple solutions of certain concentrations (5–0.25 mg/L) of MB were prepared. Then, their absorbance was measured at 665 nm by a V-730 UV-Jasco spectrophotometer, and relating each concentration with its corresponding absorbance a calibration curve was designed. For the adsorption experiments, a solution containing 1 mg/L of MB was prepared, and around 0.5 g of dry samples were introduced in 15 mL of this solution, keeping them at room temperature and static regimen for 24 h. The percentage of MB removal was also calculated by means of Eq. (1) after the concentrations of the initial and final dissolutions were determined by the calibration curve:

$$P(\%) = \frac{C_0 - C_{eq}}{C_0} \cdot 100 \quad (1)$$

where P is the equilibrium adsorption rate of the hydrogel, C_0 is the initial dye concentration, C_{eq} is the dye concentration at equilibrium.

The adsorption performance was similarly calculated by Eq. (2).

$$Q_e\left(\frac{mg_{MB}}{g_{HG}}\right) = \frac{C_0 - C_{eq}}{m} \cdot V \quad (2)$$

where V is the total volume of dye employed for each sample and m is the dry weight of the hydrogel and the rest of the variables are the same as the ones defined for Eq. (1) [13].

2.6. Antifungal studies

The antifungal activity of the extracted lignins and hydrogels was measured according to the methods previously reported by Salaberria et al. (2017) and Da Silva et al. (2018) with slight modifications [14,15]. Briefly, after culturing the mould fungus *Aspergillus niger* (CBS 554.65) on Petri dishes covered with PDA for 7 days at 25 °C ± 1.5 °C in a climatic chamber, some spores were diluted in a PBS dissolution and its concentration was adjusted to around 1.21 × 10^6 spores/ml using an automatic cell counter for the measurements (Cellometer® Mini, Nexcelom Bioscience LLC). Then, the procedure was varied according to the type of sample.

The lignins were firstly dissolved in DMSO (around 75–100 mg/mL) and then, 40 μL of the sample dissolution was poured on a Petri dish covered with PDA and the fungal strain was sprayed around. The blank was performed with DMSO [15].

In the case of the hydrogels, square portions (approximately 1 cm × 1 cm) of each sample were introduced into the PDA covered Petri dishes after having inoculated them with fungal strain. The blank was performed using neat PVA hydrogel portions.

All the tests were done by duplicate. After 7 days of incubation at 25 °C ± 1.5 °C, the lignins were evaluated visually using a numerical scale reported by da Silva et al. (2018) in accordance with ISO 846, whereas the hydrogels were extracted from the agar and washed with 1 mL of PBS in order to collect the spore solution into an Eppendorf. Afterwards, these solutions were tinged blue with 5 μL trypan blue solution and after shaking them, their spore concentration was determined with the abovementioned cell counter [14]. The fungal growth inhibition (FGI) of the samples were calculated through the equation given by Salaberria et al. (2017) [14].

3. Results and discussion

3.1. Lignin characterization

3.1.1. Purity

So as to analyse the selectivity of the lignin extraction processes, the purity of the lignin samples together with the amount of impurities that had precipitated with them was determined by quantitative acid hydrolysis. The measured purities for the obtained lignins were calculated taking the Klason lignin and acid soluble lignin (ASL) into account.

As shown in Table 3, the purity results were, in general, higher for organosolv lignins than for alkaline ones. These results are related to the selectivity of organosolv extractions [16]. It was also observed that the organosolv lignins without autohydrolysis (AOL and WOL) had purities over 90%, whereas the ones for alkaline lignins were lower than 59%. However, after autohydrolysis, the purities for the latest increased up to 88–95% while for the organosolv ones this increment was just of a 3–5%. Therefore, it can be said that autohydrolysis greatly improves the purity of the extracted lignins, especially in alkaline processes, because of the effective prior elimination of hemicelluloses, which are the main impurities after lignin extraction as demonstrated by Dávila et al. (2017). The obtained results are consistent with those reported previously [7,10].

3.1.2. Composition of the lignins

Pyrolysis-Gas Chromatography/Mass Spectrometry (Py-GC/MS) analyses were performed in order to study the composition of the eight different lignins. The resulting pyrograms are shown in Fig. 1. The numbered peaks correspond to lignin-derived phenolic compounds with

Table 3
Summary of the purity, GPC, TPC and TGA results for the isolated lignins.

Lignin sample	Purity (%)	M_w[a] (g/mol)	M_n[b] (g/mol)	M_w/M_n[c]	TPC (% GAE[d])	T_{max}[e] (°C)
AAL	58.2	4770	1109	4.3	13.8	307
AOL	90.4	8301	1072	7.8	15.6	389
WAL	49.4	4761	1054	4.5	10.6	295
WOL	92.7	6371	1246	5.1	16.5	388
AAAL	88.2	12,793	1528	8.4	33.1	355
AAOL	95.2	9020	1520	5.9	26.2	357
AWAL	95.7	16,670	1604	10.4	33.8	354
AWOL	95.2	7644	1359	5.6	27.2	365

[a] M_w: weight average molecular weight.
[b] M_n: number average molecular weight.
[c] M_w/M_n: polydispersity index.
[d] % GAE: percentage of gallic acid equivalents.
[e] T_{max}: maximum degradation temperature from TG/DTGA curves.

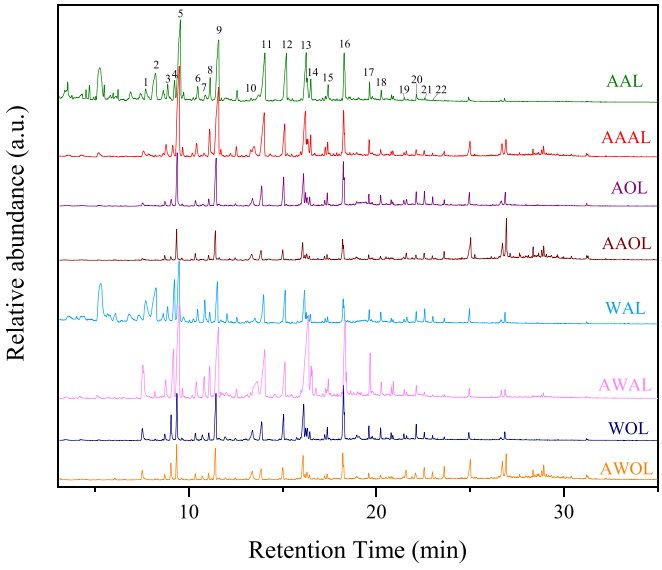

Fig. 1. Pyrograms of the extracted lignins.

larger area than 1% in at least one of the lignin samples, and their identification is displayed in Supplementary data. The untagged peaks at early times (3–7 min) mainly corresponded to degradation compounds from impurities. Furfural, for instance, was one of these compounds coming from carbohydrates and it appeared at minute 5 [10]. These impurities were especially visible in AAL and WAL samples, which also presented the lowest purity values in Table 3. From minute 23 on, the majority of the compounds with large areas were fatty acids, which are characteristic of nuts [17]. Thus, the identified compounds were detected in the range of 7–23 min and they were grouped based on the origin of their aromatic structure (*p*-hydroxyphenyl (H), guaiacol (G) and syringol (S)) [7,10].

Among the identified compounds, guaiacol (peak #5), 4-methylguaiacol (peak #9), syringol (peak #13) and 4-methylsyringol (peak #16) were the most abundant ones in all the lignin samples, constituting the 15%, 13.7%, 11.8% and 10.8% of the tagged compounds, subsequently. 4-ethylguaiacol and 4-vinylguaiacol (peaks #11 and #12, respectively) were also present in large amounts in all the samples. The compounds coming from the *p*-hydroxyphenyl unit such as phenol, *p*-cresol and *p*-ethylphenol seemed to be more abundant in WNS lignins (peaks #1, #3 and #4).

Regarding the estimated S/G ratios, all the samples presented more G units except for WOL and AWOL samples. This means that almost all the S/G ratios were below 1. However, an increase of this ratio was observed for the samples from the double-step process, which will be further studied so as to find a consistent explanation However, these values are quite different to the ones reported previously for AS and WNS lignins [7,10], which could be related to any possible modification on the composition of the feedstock or in the extraction process.

3.1.3. Average molecular weight analysis

From the GPC analyses, based on the molecular weight distributions of the lignin samples, their number-average (M_n) and weigh average (M_w) molecular weights were determined and their polydispersity indexes (M_w/M_n) were estimated. These values are displayed in Table 3.

The lignins after autohydrolysis presented higher weight and number average molecular weights in all cases. In addition, the organosolv lignins without autohydrolysis presented higher M_w than the alkaline ones, whereas for the lignins with autohydrolysis, the opposite behaviour was observed. A similar trend was perceived for the polydispersity indexes. It should also be noticed that the M_w for all the organosolv lignins was very alike, whereas for the alkaline lignins this difference was huge. However, and looking at the purity percentages and previous works [18], these results make us believe that the analysed lignin fractions for AAL and WAL were not representative of the whole lignin samples; in other words, there were probably bigger chains than 0.40 μm (which is the pore size of the used filter) that were excluded from the analysis. These would explain such enormous difference in M_w reported for alkaline lignins with and without autohydrolysis.

Some authors also reported small variations on the molecular weights of organosolv lignins from solids with and without an autohydrolysis process [19,20]. In addition, they reported that autohydrolysis permitted the obtaining of lower polydispersity indexes for organosolv lignins [19,20], as happened in the present work.

Although it is hard to find previous research on the comparison of alkaline delignification treatments with and without a prior hydrothermal treatment, the results for alkaline lignins in Table 3 are aligned with those reported in literature [10,16,21].

3.1.4. Total phenolic content (TPC)

The phenolic hydroxyl groups in the structure of lignins are usually related to its antioxidant capacity as well as to its suitability for the synthesis of new materials [22]. Therefore, it is important to study the TPC of the lignin samples. Looking at the results, it was observed that the values for the lignin samples coming from the direct delignification of the raw material (AAL, AOL, WAL and WOL) were considerably lower than those reported for the ones coming from the two-step process (AAAL, AAOL, AWAL and AWOL), which could be related to their purities [22]. It was also appreciated that AAL and WAL presented slightly lower TPC values than AOL and WOL, and they were aligned with the results obtained by García et al. (2012, 2017) and Sequeiros et al. (2014) for soda lignin [23–25]. Nevertheless, the TPC of organosolv lignins (AOL and WOL) were significantly lower than those reported by other authors [23,24,26]. As commented, the lignin samples obtained after a prior autohydrolysis process, presented significantly greater percentages of GAE (26.2–33.8% GAE). A comparable behaviour was reported by Dávila et al. (2019) for alkaline lignin extracted from pre-treated and non-treated vine shoots [22], suggesting that a prior hydrothermal treatment can be crucial to obtain high total phenolic contents in lignin. In this case, alkaline lignin samples (AAAL and AWAL) presented higher TPC values than the ones obtained for organosolv lignins. These results are in agreement with the ones reported previously for almond shells [10]. Other authors purified lignins coming from the direct delignification of the feedstock with an acid hydrolysis; nonetheless, they reported much lower GAE percentages in the purified samples than in the original ones [23,24,27]. This fact also supports the idea of subjecting the raw material to a hydrothermal pre-treatment if high TPC values want to be achieved.

3.1.5. Thermal degradation analysis (TGA)

The thermal stability of lignins is also an important characteristic to take into account, especially for their use in the production of composite materials. Thus, the thermal degradation of the extracted lignins was studied. The TGA curves are shown in Supplementary data. The maximum degradation temperatures of the samples are displayed in Table 3. All the samples had a common initial degradation step below 100 °C, corresponding to moisture evaporation. The second degradation step was the maximum degradation stage for all the samples. However, the temperatures differed depending on the lignin extraction. In fact, for the alkaline lignins obtained though a single-step process (AAL and WAL), the maximum degradation happened around 300 °C, whereas for the organosolv lignins this temperature was significantly higher (≈390 °C). This could be ascribed to their high amount of impurities as well as to the fractions with low molecular weight [21,28], as reported in Section 3.1.3. The lignins coming from the double-step processes presented similar maximum degradation temperatures (354–365 °C), which were within the ones reported for single-step process lignins and were in accordance with previous results [10]. In this temperature

range, the scission of β–O–4 ether bondages tend to occur, followed by the division of C—C linkages and aromatic rings [28].

A third degradation stage was observed around 420 °C, although this temperature was again lower for AAL and WAL (≈390 °C) samples and higher for AOL and WOL samples (≈ 470 °C). The latest then presented a constant weight loss until 37% of their initial weight. The rest of the samples presented a fourth degradation step around 700 °C, leading to a final residue between 20 and 29% of their initial weight. This last stage could be related to the demethoxylation or condensation reactions of the volatile products of lignin [28], and the amounts of residue were aligned with those reported previously [10].

3.1.6. Crystallinity

The XRD patterns of the lignin samples are depicted in Fig. 2. As shown, all the organosolv lignins and the alkaline ones coming from the double-step processes (AAAL and AWAL), presented the typical broad signal around 2θ = 22°, representing its amorphous structure [29]. AAL and WAL samples presented narrower peaks at the same diffraction angle. Moreover, they also presented sharp signals at 11, 12, 19, 25 and 31°, which are more characteristic of the crystalline domains of cellulose [30,31] and hemicelluloses [32]. Therefore, an important presence of impurities in these lignins was again confirmed by XRD analysis, leading to a modification on the ordered domains.

3.1.7. Chemical structure

The main functional groups of the isolated lignins were determined by FTIR technique (Figure 3). Although all the recorded spectra presented the typical lignin bands [7,22,26], the intensities of some of them changed from sample to sample. Some of these variations were observed in the range 2827–2998 cm^{-1}, which corresponded to the C—H (CH_3, CH_2 and CH) stretching vibration of lignin and polysaccharides [19], and were more notable for alkaline lignin samples, probably due to the lower elimination of sugars during the autohydrolysis step. Before the footprint range, at 1650 cm^{-1}, a peak corresponding to conjugated C═O stretching vibration [19] was detected for the single-step lignins, but it disappeared after the autohydrolysis step. Although some authors have previously related this band to alkaline processes [33], it may be attributed to the presence of impurities in AAL, WAL, AOL and WOL lignins. On the footprint range (1500–600 cm^{-1}) the main changes were seen on the intensity of the bands. AAL and WAL samples, for instance, presented a clear decrease on the intensity of the bands ascribed to the condensed syringil or guaiacyl unit breathing (1325 cm^{-1}) [34,35] and aromatic methyl ethers of lignin (1215 cm^{-1}) [19]. Conversely, the peaks at 1157, 1080, 975 and 896 cm^{-1}, corresponding to C—O stretching vibration in ester groups [34,35], C—O deformation in secondary alcohol and aliphatic ethers, —HC═CH out-of-plane and C—H deformation vibrations [35], subsequently, got intensified in the aforementioned samples. The remaining bands were similar for all the lignin samples, confirming the existence of syringyl and guaiacyl units in all the lignins, although their ratios were different, as demonstrated in Section 3.1.2.

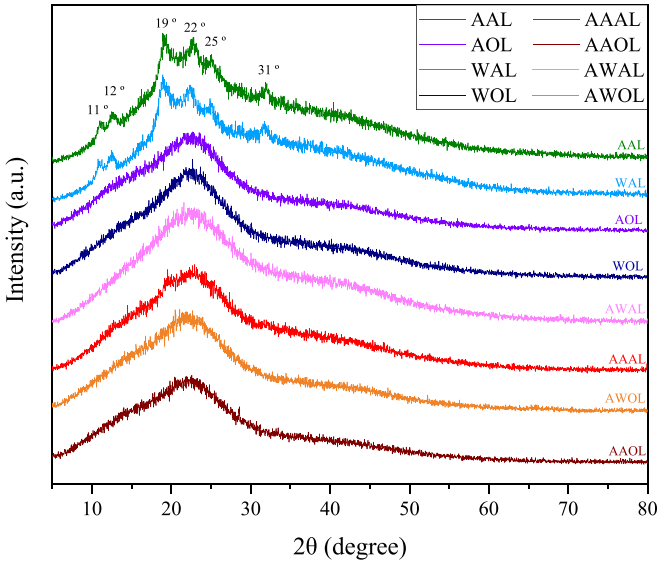

Fig. 2. XRD patterns of the extracted lignins.

3.2. Hydrogel characterization

3.2.1. Lignin waste

The lignin waste of the samples was analysed so as to determine their final lignin content. The results are shown in Table 4. For the samples made from alkaline lignin, the ones containing lignins from the single-step processes (AA and WA) presented higher lignin wastes than the ones containing lignins coming from double-step processes (AAA and AWA). A similar trend was observed for organosolv lignins from WNS (WO and AWO), whereas for the ones coming from AS (AO and AAO) the reported behaviour was the opposite. This might be related to the polidispersity of the lignins, since except for AOL and AAOL, the polydispersity of the rest of the lignins increased from single to double-step lignins. This fact suggests that highest molecular weight lignin chains might have been able to interact with the PVA matrix, whereas lowest molecular weight fractions were eliminated. However, further studies should be done in order to verify this statement. Moreover, lower waste percentages were accounted for AS lignins than for WNS lignins in the case of the single-step lignins (56.2–66.5% vs. 60.0–68.5%), while for the double-step lignins the contrary was appreciated (44.2–59.9% vs. 59.6–71.1%). These values are in great accordance with those reported previously [13]. It should also be noted that among the single-step lignin containing samples the ones with alkaline lignin showed greater lignin wastes that the ones containing organosolv lignin, whereas the samples with double-step lignins exhibited the inverse trend.

In addition, the samples with a long last thawing step, in general, presented lower lignin waste values, suggesting that the lengthening of the last cycle may have enhanced the interactions between the PVA and the lignin. Furthermore, the samples with single-step alkaline WNS lignin (WA) showed a significant reduction on their lignin waste. On the contrary, the samples with double-step alkaline WNS lignin (AWA) presented much greater lignin waste values than those reported before. It can also be said that, except for AWA sample, all the alkaline lignin containing hydrogels lost less lignin than the ones containing organosolv lignin.

3.2.2. Swelling

As the swelling capacity of the hydrogels is determining for assessing their applications, this property was measured for all the samples and it is displayed in Fig. 4.

The samples with short last thawing cycle presented swelling values between 336 and 505%, which corresponded to AWO and WA samples, respectively. Moreover, the samples containing alkaline lignin showed in all cases higher swelling capacities, which is in accordance with the data reported previously [13], which could be related to the attachment of the fractions with highest molecular weights to the matrix. Comparing the aforementioned samples with the ones with a long last thawing stage, a huge enhancement of this property was clearly seen. The most significant improvement (80% more regarding its prior swelling ability) was seen on AWO sample, which was the one that had previously presented the lowest swelling capacity. On the contrary, the sample that exhibited the slightest enhancement was AWA, whose swelling ability was just improved about 22%. Agudelo et al. (2018) studied the influence of various synthesis parameters such as the time of the freeze-thawing cycles on the swelling capacity of neat PVA hydrogels [36]. According to their work, the excessive lengthening of the thawing cycles

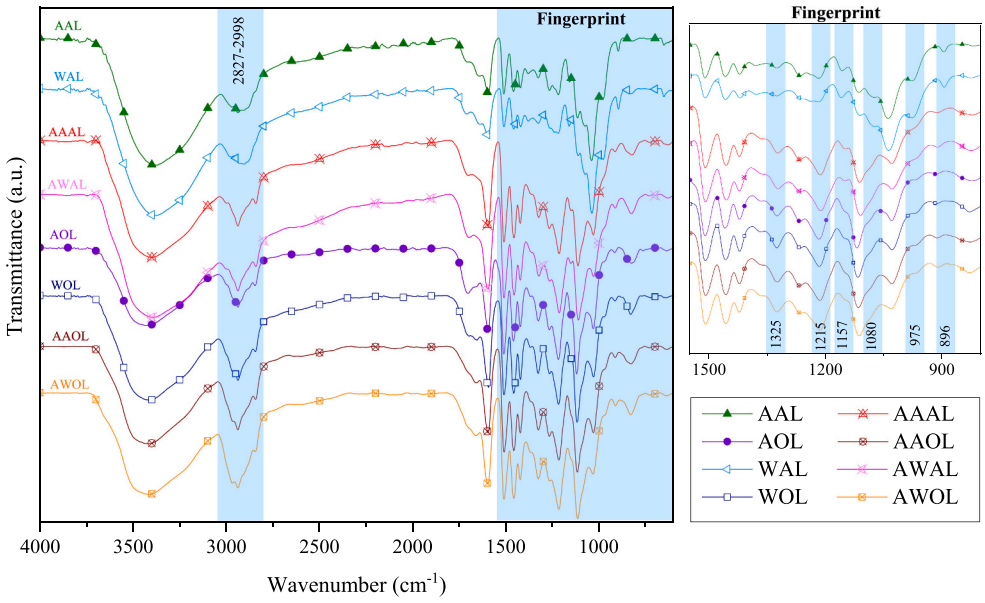

Fig. 3. FTIR spectra of the extracted lignins.

Table 4
Lignin waste (%) of the analysed short (SC) and long (LC) last thawing step samples.

Sample	SC (%)	LC (%)
AA	66.5 ± 2.9	48.5 ± 3.0
AO	56.2 ± 2.4	53.9 ± 3.4
WA	68.5 ± 0.7	26.0 ± 6.4
WO	60.0 ± 1.8	53.9 ± 2.1
AAA	59.6 ± 2.8	36.3 ± 2.0
AAO	71.1 ± 3.0	48.1 ± 3.3
AWA	44.2 ± 1.6	74.3 ± 3.7
AWO	59.9 ± 4.0	51.7 ± 2.2

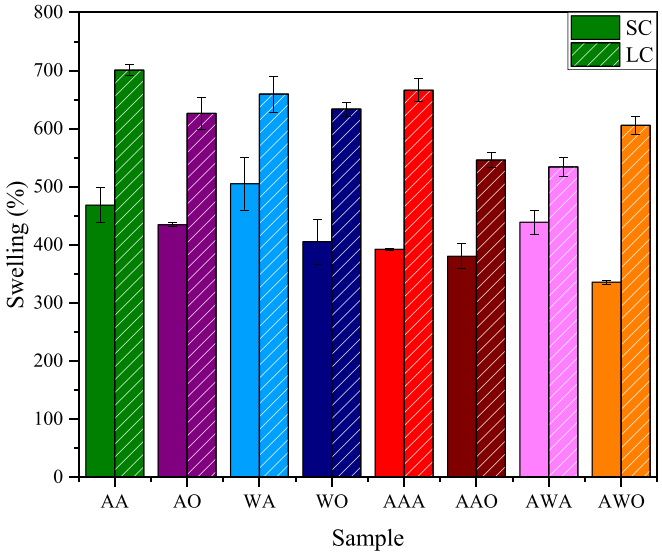

Fig. 4. Swelling capacity of the synthesized hydrogels with short (SC) and long (LC) last thawing steps.

leads to the dissolution of the formed crystallites, which reduces of their quantity and size and, hence, also the crosslinking density and the swelling capacity of the hydrogel [36]. Thus, as in the present work the lengthened thawing step was the last one, the molten crystallites might have evaporated, reducing the crosslinking density of the samples and resulting in a notable enhancement of their swelling capacity. Nevertheless, this phenomenon should be further investigated in order to find a more reliable explanation.

It should also be mentioned that the samples containing lignins coming from single-step processes, presented higher swelling capacities than the ones coming from the double-step processes, probably due to the interactions of their impurities with the polymeric matrix. Although Wu et al. (2019) related the swelling properties to the content of phenolic hydroxyl groups and to the molecular weight of the employed lignins, their hypothesis would not explain the behaviour of the hydrogels in this work [12]. In fact, the samples containing lignin with the lowest total phenolic contents and lowest average molecular weights (AA and WA) presented the highest swelling capacities. However, this might support the previous statement about the non-representative average molecular weights determined for these lignins (Section 3.1.3) and also the one about the interactions with non-lignin components (Section 3.2.1), since these samples presented high lignin wastes.

3.2.3. *Morphology*

The morphology of the synthesized hydrogels was studied by Scanning Electron Microscopy (SEM). The corresponding micrographs for the samples containing AS lignins at 500× and 5000× magnifications are shown in Fig. 5 and the ones for WNS lignin samples in Supplementary data.

At first sight, it was seen that all the hydrogels presented different appearances. Although all the samples presented porous structures at different levels, their distribution, size and density was distinct. In fact, all the samples that corresponded to hydrogels containing lignins from single-step processes were quite similar and presented a highly porous honeycomb structure, as expected for lignin containing PVA hydrogels [13,37–39]. Their pore sizes and distributions were quite homogeneous, but the walls between the micro voids were smoother and more brittle in the case of AA and WA samples than in AO and WO samples, which presented thicker walls. These structures were responsible for their high water absorption capacities [40] and could have been created due to the interactions of PVA with the highest molecular weight lignin fractions.

When lignins from the double-step processes were employed, the synthesized hydrogels displayed much denser and continuous structures with hardly recognizable pores, which may be related to a higher

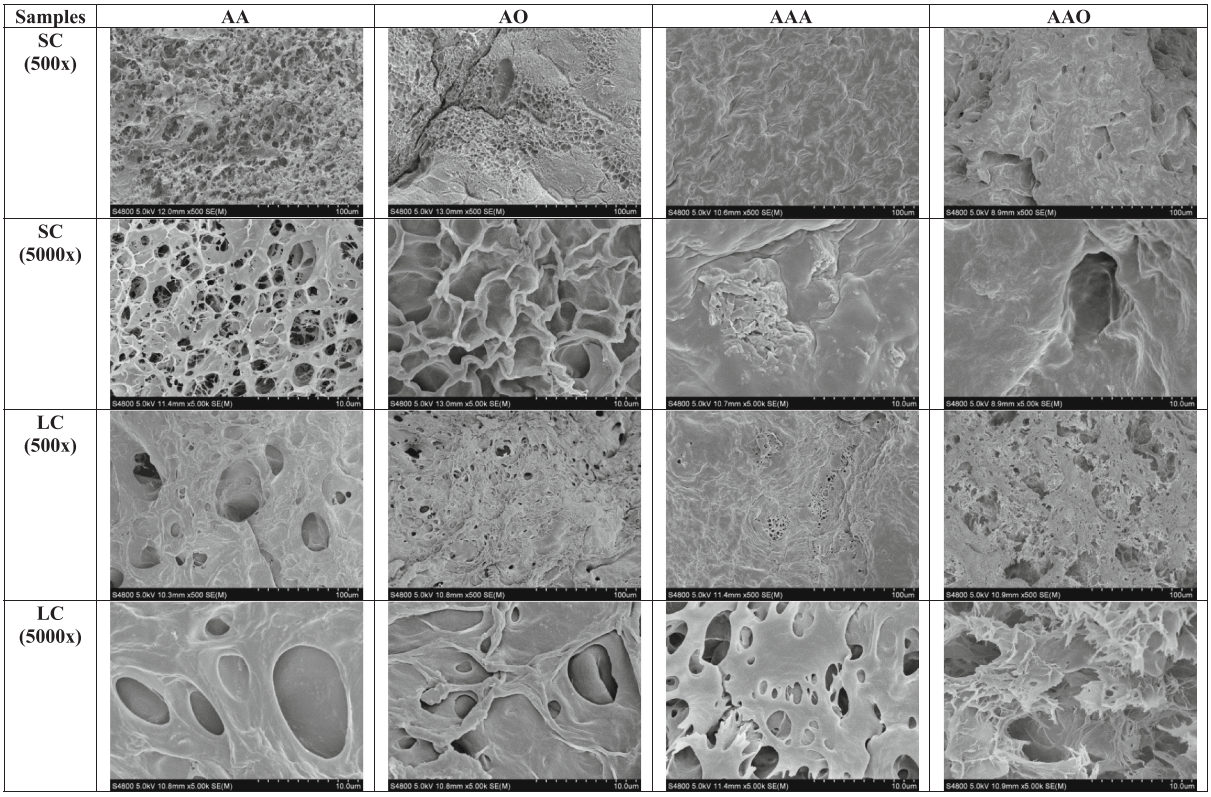

Fig. 5. SEM micrographs of the hydrogels containing AS lignins at 500× and 5000× magnifications.

crosslinking density with these lignins due to their higher contents in phenolic hydroxyl groups [12]. Rachip et al. (2013) also reported variable hydrogel morphologies according to the —OH and —COOH groups in lignin [41]. These microstructures would explain the drop on the swelling ability of the present samples compared to the aforementioned ones.

It was also appreciated that when the last thawing step was lengthened, there was an evident creation of macro pores in all cases. As aforementioned, this might be ascribed to the evaporation of molten crystallites during the last step of the synthesis, which permitted the formation of these structures and improved the swelling performance of all the hydrogels, regardless of their origin or extraction type.

Although the influence of the number of cycles has been previously studied by many authors for freeze-thawed PVA hydrogels [13,36,40,42,43], the duration of last thawing step has not been investigated. So, the present study could pave the way to new synthesis routes since it offers a simple way of enhancing the swelling capacity of the samples.

3.2.4. Glass transition temperature

The glass transition temperature (T_g) is an important characteristic of polymeric materials since it determines their applicability. Thus, the synthesized hydrogels were subjected to Differential Scanning Calorimetry (DSC) analyses and the results are presented in Table 5.

The samples containing alkaline lignins presented higher T_g values ranging from 72 to 91 °C whereas the ones containing organosolv lignins showed lower T_g values (69–86 °C). The highest T_g values were found for AA and AAA samples (≈91 °C), which might be because the impurities could have acted as bridges between the PVA and the lignin chains, enhancing their interactions and hindering the relaxation and arrangement of the chains [41,44]. On the contrary, although WA sample contained lignin with a higher amount of impurities, part of the latest might have dissolved in the aqueous phase, being washed out during the washing step and, hence, being unable to enhance the interactions between PVA and lignin. Therefore, in this case, the T_g value was lower.

Table 5
Glass transition temperatures (T_g) and compression modules of the synthesized hydrogels after short (SC) and long (LC) last thawing steps.

Sample	T_g (°C)		Compression module (MPa)		MB removal (%)	
	SC	LC	SC	LC	SC	LC
AA	91.0	77.3	16.3 ± 1.8	10.8 ± 3.2	79.5 ± 3.6	81.3 ± 1.8
AO	73.0	66.6	5.0 ± 1.9	2.1 ± 0.7	90.3 ± 0.6	83.4 ± 2.8
WA	79.0	64.0	14.9 ± 1.9	13.6 ± 0.8	75.3 ± 3.7	82.3 ± 3.0
WO	69.7	77.7	6.0 ± 1.0	2.0 ± 0.8	89.6 ± 1.0	86.9 ± 4.4
AAA	91.1	66.6	13.1 ± 0.8	7.5 ± 2.7	86.6 ± 3.2	93.3 ± 1.1
AAO	85.8	82.8	2.1 ± 1.0	2.0 ± 0.8	90.1 ± 2.2	87.1 ± 6.7
AWA	72.1	66.4	6.6 ± 2.9	6.4 ± 1.3	87.9 ± 3.6	86.9 ± 5.5
AWO	70.8	92.2	5.4 ± 2.8	2.88 ± 1.2	93.0 ± 0.6	88.6 ± 1.9

Except for AWA sample, the hydrogels containing double-step lignins presented higher T_g values than the ones with single-step lignins, which also matched with the previously reported drop on their swelling capacity due to a higher crosslinking degree between lignin and PVA. However, this could also be attributed to the increment on the average molecular weights of the lignins as well as to their total phenolic content. These two factors affect the total —OH groups of lignin, which although according to Raschip et al. (2013) seemed to decrease the T_g of pure lignin, they could have enhanced the hydrogen bonding with the matrix polymer, making its chains flow at higher temperatures [41].

When the last thawing step was lengthened, all the T_g values dropped except for WO and AWO samples. This might have occurred due to an increment on the interactions between lignin and PVA after water evaporation due to the rearrangement of WO and AWO chains, which presented low average molecular weights and the lowest polydispersities. Thus, the resulting hydrogels were more thermally stable. Nevertheless, to the best of our knowledge there is no literature that supports and explains this fact.

3.2.5. Compression tests

The mechanical performance of the hydrogels was studied compressing them up to the 80% of their initial thickness. From the obtained stress-strain diagrams, the compression modules were calculated, as displayed in Table 5. As in the previous work, at the end of the tests none of the tested hydrogels was fractured and showed excellent recoverability. Nevertheless, the samples containing alkaline lignin from the single-step processes were slightly damaged due to their heterogeneous appearance.

The aforementioned samples (AA and WA) were the ones presenting the highest compression modules (14.8 and 16.3 MPa, respectively) although they were also the ones with the highest swelling ability, which might be related to the formed honeycomb structures due to the interactions of the matrix with lignin and its impurities, as shown in Section 3.2.3. In spite of their analogous morphology, the samples containing single-step organosolv lignins (AO and WO) presented much lower compression modules (4.95 and 6.01 MPa, respectively). A similar behaviour was observed for the samples composed of double-step lignins: the ones with alkaline lignin presented higher compression modules (6.63–13.07 MPa) than the organosolv ones (2.05–5.4 MPa).

The modules of all the samples presented a slight drop when increasing the duration of the last thawing step, probably due to the creation of the macro pores, as aforementioned. This trend was also aligned to the one observed for T_g values. All the estimated modules were in great accordance with previous results [13], and were higher than those reported by other authors for lignin-based hydrogels [1,45].

3.3. Methylene blue adsorption studies

So as to study the applicability of the designed hydrogels as dye adsorbents, methylene blue (MB) adsorption tests were performed following the procedure described before [13]. It is known that thanks to interactions of the multiple negative charges on the surface of lignin-hydrogels, these materials are able to capture positively charged compounds such as cationic dyes [12,13], which are also employed in many medical applications [46].

As displayed in Table 5, it was demonstrated that the synthesized samples presented great potential for MB adsorption for the tested solution, being the lowest removal value 75% and the highest 93% of the pollutant, which exceeded in both cases previous results [13]. In general, the samples containing double-step lignins were able to trap larger quantities of dye, and the alkaline lignin-based hydrogels removed slightly lower values of MB than the organosolv-based ones, which is also in line with the trend reported for the TPC of the lignins. Dominguez-Robles et al. (2018) also reported lower MB adsorption values for their samples containing soda lignin than for the ones with organosolv lignin, which could be related with the values they reported for the phenolic hydroxyl groups in these lignins [11]. In contrast, when the last thawing cycle was lengthened, the MB adsorption capacity of the samples containing alkaline lignins was enhanced whereas the MB removal of organosolv lignin-based hydrogels got slightly reduced. This fact suggested that although the last thawing cycle intensified the porosity of the samples, the availability of the negative charges on the surface was altered; nevertheless, this statement cannot be demonstrated.

In spite of the removal values being very high, it is true that the yield of the adsorption tests was much lower than in other studies. Whereas values from 2 to 200 mg dye/g hydrogel have been previously reported for lignin hydrogels [11,47–49], in this work none of the synthesized hydrogels surpassed 0.1 mg dye/g hydrogel. Furthermore, in recent years biochars have been used for the removal of these dyes, which far exceed the yields reported in this work [11,50]. Thus, the present hydrogels could be used for diluted MB environments, and modifications could be studied together with the combination with other compounds in order to enhance the adsorption yields.

3.4. Antifungal tests

The urgent need of searching for alternative eco-friendly materials has also swayed the food-packaging sector. In this context, bio-based hydrogels have emerged as potential absorbents for these systems [51]. However, these materials should extend the shelf-life of the packaged products, which involves hindering the growth of microorganisms and fungi on them [51,52]. Thus, the antifungal properties against *Aspergillus niger* (brown-rot fungi), one of the most common fungi in food spoilage, were studied for all the synthesized hydrogels.

First of all, a visual evaluation of lignin's antifungal capacity was performed (see Supplementary data). Although mainly white-rot fungi are able to depolymerise lignin [53], some authors have also seen that brown-rot fungi are also capable to be lignin degraders. Nevertheless, in this case the tested fungi did not seem to have such ability. In spite of the growth of fungi the agar surface of all the samples, the deposited lignin drops could be clearly observed after the period of the test. This showed the antifungal ability of lignin, as also demonstrated by other authors before. Among the studied samples, the alkaline ones seemed to be able to inhibit more effectively the fungal growth than the organosolv ones, leading to a growth intensity of 3 (GI = 3), whereas most of the rest of the samples presented greater intensities (GI ≈ 4), according to ISO 846 [15].

On the other hand, the same test was performed to the hydrogels. In all cases, the whole hydrogel portion was visible after the test (see Supplementary data). At first sight, the samples with alkaline WNS lignins (WA and AWA) as well as the samples containing organosolv AS lignins (AO and AWO) seemed to hinder the fungal development more than the samples containing other lignins. Moreover, there was almost no appreciable fungal growth on the top surface of the samples. In this case, the growth intensity would be between 3 and 4 for every sample [15].

The samples were washed with PBS and the surrounding spores were quantified as aforementioned. From the estimated FGI values (Fig. 6), it was seen that among the studied samples, the ones presenting the lowest fungal activity were WO and AAO (58 and 56.5% FGI, respectively), and the one presenting the highest growth was surprisingly AWA (almost 40% more than the control sample). It was observed that the samples containing single-step AS lignins presented lower FGI values than the ones with double-step AS lignins. Conversely, the samples containing double-step WNS lignins presented worse antifungal activity than the ones with single-step WNS lignins. Although the estimated values were approximate, these results helped making an idea of the antifungal properties that the synthesized samples presented. It is also worth to mention that none of the studied samples lost weight during the

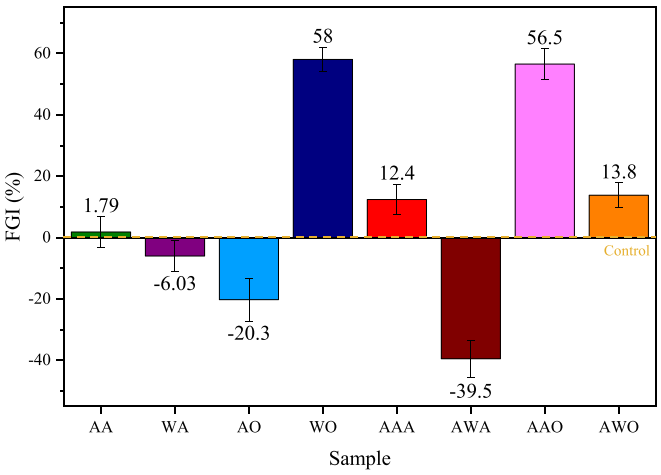

Fig. 6. Fungal growth inhibition (FGI, %) of the samples with respect to the control hydrogels (y = 0).

antifungal test, which supports their effectiveness against *A. niger*.

Several authors have reported similar FGI values for other materials for food packaging applications. For instance, Salaberria et al. (2017) reported 52–62% of inhibition for PLA films containing functionalized chitin nanocrystals [14]. In the study of Fernandez-Marin et al. (2021), these values were between 72 and 86% for their chitosan/β-chitin nanofibers nanocomposites due to the incorporation of deterpenated *Origanum majorana* L. essential oil [54]. Conversely, Dey et al. (2021) reported values between 51 and 56% for neat PVA films, which were negatively affected by the addition of cellulose nanocrystals and chitosan nanoparticles [55]. Thus, taking these data into account, it can be concluded that the results reported for WO and AAO hydrogels were in total agreement with the ones reported by other authors and could be employed in food packaging.

4. Conclusions

In this study, alkaline and organosolv lignins were extracted from almond and walnut shells through two different biorefinery strategies and successfully employed for the synthesis of lignin-based physical hydrogels. The characterization of the extracted lignins showed significant differences between the lignin samples, especially on their composition, average molecular weights and total phenolic contents. As expected, the autohydrolysis enhanced the purity of the lignins, especially in the case of alkaline ones, and it also promoted the extraction of lignins with higher average molecular weights. These changes altered the morphology of the produced hydrogels and, hence, their properties such as their swelling capacity, glass transition temperatures and compression modules. In fact, hydrogels containing lignins from the single-step process resulted into a more honeycomb porous structure and, thus, a higher water absorption capacity. In addition, when the last thawing step was lengthened, larger pores were created, which also leaded to a notable enhancement of the swelling percentage of the hydrogels. The synthesized materials showed good methylene blue removal (75–93%) and, in some cases, antifungal properties (up to 58% of FGI), demonstrating their versatility on various application fields.

Declaration of Competing Interest

The authors declare that they have no known competing financial interests or personal relationships that could have appeared to influence the work reported in this paper.

Acknowledgements

The authors would like to acknowledge the financial support of the Department of Education of the Basque Government (IT1008-16). A. Morales would like to thank the University of the Basque Country (Training of Researcher Staff, PIF17/207). P. Gullón would like to acknowledge the Grants for the recruitment of technical support staff (PTA2019-017850-I) under the State Plan for Scientific and Technical Research and Innovation 2017–2020. The authors thank SGIker (UPV/EHU/ERDF, EU) for their technical and human support.

Appendix A. Supplementary data

Supplementary data to this article can be found online at https://doi.org/10.1016/j.susmat.2021.e00369.

References

[1] R.M. Kalinoski, J. Shi, Hydrogels derived from lignocellulosic compounds: evaluation of the compositional, structural, mechanical and antimicrobial properties, Ind. Crop. Prod. 128 (2019) 323–330, https://doi.org/10.1016/j.indcrop.2018.11.002.

[2] D. Rico-García, L. Ruiz-Rubio, L. Pérez-Álvarez, S.L. Hernández-Olmos, G. L. Guerrero-Ramírez, J.L. Vilas-Vilela, Lignin-based hydrogels : synthesis and applications, Polymers (Basel). 12 (2020) 1–23.

[3] A. Oryan, A. Kamali, A. Moshiri, H. Baharvand, H. Daemi, Chemical crosslinking of biopolymeric scaffolds: current knowledge and future directions of crosslinked engineered bone scaffolds, Int. J. Biol. Macromol. 107 (2018) 678–688, https://doi.org/10.1016/j.ijbiomac.2017.08.184.

[4] H. Nakajima, P. Dijkstra, K. Loos, The recent developments in biobased polymers toward general and engineering applications: polymers that are upgraded from biodegradable polymers, analogous to petroleum-derived polymers, and newly developed, Polymers (Basel). 9 (2017) 1–26, https://doi.org/10.3390/polym9100523.

[5] S. RameshKumar, P. Shaiju, K.E. O'Connor, P. Ramesh Babu, Bio-based and biodegradable polymers - state-of-the-art, challenges and emerging trends, Curr. Opin. Green Sustain. Chem. 21 (2020) 75–81, https://doi.org/10.1016/j.cogsc.2019.12.005.

[6] A.T. Ubando, C.B. Felix, W.H. Chen, Biorefineries in circular bioeconomy: a comprehensive review, Bioresour. Technol. 299 (2020), https://doi.org/10.1016/j.biortech.2019.122585.

[7] A. Morales, J. Labidi, P. Gullón, Hydrothermal treatments of walnut shells: a potential pretreatment for subsequent product obtaining, Sci. Total Environ. 764 (2021), 142800, https://doi.org/10.1016/j.scitotenv.2020.142800.

[8] G. Dragone, A.A.J. Kerssemakers, J.L.S.P. Driessen, C.K. Yamakawa, L.P. Brumano, S.I. Mussatto, Innovation and strategic orientations for the development of advanced biorefineries, Bioresour. Technol. 302 (2020), 122847, https://doi.org/10.1016/j.biortech.2020.122847.

[9] J.J. Liao, N.H.A. Latif, D. Trache, N. Brosse, M.H. Hussin, Current advancement on the isolation, characterization and application of lignin, Int. J. Biol. Macromol. 162 (2020) 985–1024, https://doi.org/10.1016/j.ijbiomac.2020.06.168.

[10] A. Morales, F. Hernández-Ramos, L. Sillero, R. Fernández-Marín, I. Dávila, P. Gullón, X. Erdocia, J. Labidi, Multiproduct biorefinery based on almond shells: impact of the delignification stage on the manufacture of valuable products, Bioresour. Technol. 315 (2020), https://doi.org/10.1016/j.biortech.2020.123896.

[11] J. Domínguez-Robles, M.S. Peresin, T. Tamminen, A. Rodríguez, E. Larrañeta, A. S. Jääskeläinen, Lignin-based hydrogels with "super-swelling" capacities for dye removal, Int. J. Biol. Macromol. 115 (2018) 1249–1259, https://doi.org/10.1016/j.ijbiomac.2018.04.044.

[12] L. Wu, S. Huang, J. Zheng, Z. Qiu, X. Lin, Y. Qin, Synthesis and characterization of biomass lignin-based PVA super-absorbent hydrogel, Int. J. Biol. Macromol. 140 (2019) 538–545, https://doi.org/10.1016/j.ijbiomac.2019.08.142.

[13] A. Morales, J. Labidi, P. Gullón, Effect of the formulation parameters on the absorption capacity of smart lignin-hydrogels, Eur. Polym. J. 129 (2020), 109631, https://doi.org/10.1016/j.eurpolymj.2020.109631.

[14] A.M. Salaberria, R.H. Diaz, M.A. Andrés, S.C.M. Fernandes, J. Labidi, The antifungal activity of functionalized chitin nanocrystals in poly (Lactid acid) films, Materials (Basel). 10 (2017) 1–16, https://doi.org/10.3390/ma10050546.

[15] D.T. Da Silva, R. Herrera, B.M. Heinzmann, J. Calvo, J. Labidi, Nectandra grandiflora by-products obtained by alternative extraction methods as a source of phytochemicals with antioxidant and antifungal properties, Molecules. 23 (2018) 1–16, https://doi.org/10.3390/molecules23020372.

[16] J. Fernández-Rodríguez, X. Erdocia, C. Sánchez, M. González Alriols, J. Labidi, Lignin depolymerization for phenolic monomers production by sustainable processes, J. Energy Chem. 26 (2017) 622–631, https://doi.org/10.1016/j.jechem.2017.02.007.

[17] C.S.G.P. Queirós, S. Cardoso, A. Lourenço, J. Ferreira, I. Miranda, M.J.V. Lourenço, H. Pereira, Characterization of walnut, almond, and pine nut shells regarding chemical composition and extract composition, Biomass Convers. Biorefin. 10 (2020) 175–188, https://doi.org/10.1007/s13399-019-00424-2.

[18] A. Morales, B. Gullón, I. Dávila, G. Eibes, J. Labidi, P. Gullón, Optimization of alkaline pretreatment for the co-production of biopolymer lignin and bioethanol from chestnut shells following a biorefinery approach, Ind. Crop. Prod. 124 (2018), https://doi.org/10.1016/j.indcrop.2018.08.032.

[19] J. Li, P. Feng, H. Xiu, J. Li, X. Yang, F. Ma, X. Li, X. Zhang, E. Kozliak, Y. Ji, Morphological changes of lignin during separation of wheat straw components by the hydrothermal-ethanol method, Bioresour. Technol. 294 (2019), https://doi.org/10.1016/j.biortech.2019.122157.

[20] M.Q. Zhu, J.L. Wen, Y.Q. Su, Q. Wei, R.C. Sun, Effect of structural changes of lignin during the autohydrolysis and organosolv pretreatment on Eucommia ulmoides Oliver for an effective enzymatic hydrolysis, Bioresour. Technol. 185 (2015) 378–385, https://doi.org/10.1016/j.biortech.2015.02.061.

[21] I. Dávila, P. Gullón, M.A. Andrés, J. Labidi, Coproduction of lignin and glucose from vine shoots by eco-friendly strategies: toward the development of an integrated biorefinery, Bioresour. Technol. 244 (2017) 328–337, https://doi.org/10.1016/j.biortech.2017.07.104.

[22] I. Dávila, B. Gullón, J. Labidi, P. Gullón, Multiproduct biorefinery from vine shoots: bio-ethanol and lignin production, Renew. Energy 142 (2019) 612–623.

[23] A. García, M. González Alriols, G. Spigno, J. Labidi, Lignin as natural radical scavenger. Effect of the obtaining and purification processes on the antioxidant behaviour of lignin, Biochem. Eng. J. 67 (2012) 173–185, https://doi.org/10.1016/j.bej.2012.06.013.

[24] A. García, G. Spigno, J. Labidi, Antioxidant and biocide behaviour of lignin fractions from apple tree pruning residues, Ind. Crop. Prod. 104 (2017) 242–252, https://doi.org/10.1016/j.indcrop.2017.04.063.

[25] A. Sequeiros, D.A. Gatto, J. Labidi, L. Serrano, Different extraction methods to obtain lignin from almond shell, J. Biobased Mater. Bioenergy. 8 (2014) 370–376, https://doi.org/10.1166/jbmb.2014.1443.

[26] S. De, S. Mishra, E. Poonguzhali, M. Rajesh, K. Tamilarasan, Fractionation and characterization of lignin from waste rice straw: biomass surface chemical composition analysis, Int. J. Biol. Macromol. 145 (2020) 795–803, https://doi.org/10.1016/j.ijbiomac.2019.10.068.
[27] I. Gómez-Cruz, M. del Mar Contreras, I. Romero, E. Castro, A biorefinery approach to obtain antioxidants, lignin and sugars from exhausted olive pomace, J. Ind. Eng. Chem. 96 (2021) 356–363, https://doi.org/10.1016/j.jiec.2021.01.042.
[28] C. Xu, F. Liu, M.A. Alam, H. Chen, Y. Zhang, C. Liang, H. Xu, S. Huang, J. Xu, Z. Wang, Comparative study on the properties of lignin isolated from different pretreated sugarcane bagasse and its inhibitory effects on enzymatic hydrolysis, Int. J. Biol. Macromol. 146 (2020) 132–140, https://doi.org/10.1016/j.ijbiomac.2019.12.270.
[29] A. Goudarzi, L.-T. Lin, F.K. Ko, X-ray diffraction analysis of Kraft Lignins and lignin-derived carbon nanofibers, J. Nanotechnol. Eng. Med. 5 (2014), 021006, https://doi.org/10.1115/1.4028300.
[30] S. Kumar, Y.S. Negi, J.S. Upadhyaya, Studies on characterization of corn cob based nanoparticles, Adv. Mater. Lett. 1 (2010) 246–253, https://doi.org/10.5185/amlett.2010.9164.
[31] A.C.F. Louis, S. Venkatachalam, Energy efficient process for valorization of corn cob as a source for nanocrystalline cellulose and hemicellulose production, Int. J. Biol. Macromol. 163 (2020) 260–269, https://doi.org/10.1016/j.ijbiomac.2020.06.276.
[32] M.K. Haider, A. Ullah, M.N. Sarwar, Y. Saito, L. Sun, S. Park, I.S. Kim, Lignin-mediated in-situ synthesis of CuO nanoparticles on cellulose nanofibers: a potential wound dressing material, Int. J. Biol. Macromol. 173 (2021) 315–326, https://doi.org/10.1016/j.ijbiomac.2021.01.050.
[33] M. Brahim, N. Boussetta, N. Grimi, E. Vorobiev, I. Zieger-Devin, N. Brosse, Pretreatment optimization from rapeseed straw and lignin characterization, Ind. Crop. Prod. 95 (2017) 643–650, https://doi.org/10.1016/j.indcrop.2016.11.033.
[34] X. Yang, Y. Zhao, H. Mussana, M. Tessema, L. Liu, Characteristics of cotton fabric modified with chitosan (CS)/cellulose nanocrystal (CNC) nanocomposites, Mater. Lett. 211 (2018) 300–303, https://doi.org/10.1016/j.matlet.2017.09.075.
[35] L. Chen, X. Wang, H. Yang, Q. Lu, D. Li, Q. Yang, H. Chen, Study on pyrolysis behaviors of non-woody lignins with TG-FTIR and Py-GC/MS, J. Anal. Appl. Pyrolysis 113 (2015) 499–507, https://doi.org/10.1016/j.jaap.2015.03.018.
[36] J.I. Daza Agudelo, J.M. Badano, I. Rintoul, Kinetics and thermodynamics of swelling and dissolution of PVA gels obtained by freeze-thaw technique, Mater. Chem. Phys. 216 (2018) 14–21, https://doi.org/10.1016/j.matchemphys.2018.05.038.
[37] X. Han, Z. Lv, F. Ran, L. Dai, C. Li, C. Si, Green and stable piezoresistive pressure sensor based on lignin-silver hybrid nanoparticles/polyvinyl alcohol hydrogel, Int. J. Biol. Macromol. 176 (2021) 78–86, https://doi.org/10.1016/j.ijbiomac.2021.02.055.
[38] Q. Wang, J. Guo, X. Lu, X. Ma, S. Cao, X. Pan, Y. Ni, Wearable lignin-based hydrogel electronics: a mini-review, Int. J. Biol. Macromol. (2021), https://doi.org/10.1016/j.ijbiomac.2021.03.079.
[39] L. Sun, Z. Mo, Q. Li, D. Zheng, X. Qiu, X. Pan, Facile synthesis and performance of pH/temperature dual-response hydrogel containing lignin-based carbon dots, Int. J. Biol. Macromol. 175 (2021) 516–525, https://doi.org/10.1016/j.ijbiomac.2021.02.049.
[40] A. Morales, J. Labidi, P. Gullón, Assessment of green approaches for the synthesis of physically crosslinked lignin hydrogels, J. Ind. Eng. Chem. 81 (2020) 475–487, https://doi.org/10.1016/j.jiec.2019.09.037.
[41] I.E. Raschip, G.E. Hitruc, C. Vasile, M.C. Popescu, Effect of the lignin type on the morphology and thermal properties of the xanthan/lignin hydrogels, Int. J. Biol. Macromol. 54 (2013) 230–237, https://doi.org/10.1016/j.ijbiomac.2012.12.036.
[42] A.H.A. Wahab, A.P.M. Saad, M.N. Harun, A. Syahrom, M.H. Ramlee, M.A. Sulong, M.R.A. Kadir, Developing functionally graded PVA hydrogel using simple freeze-thaw method for artificial glenoid labrum, J. Mech. Behav. Biomed. Mater. 91 (2019) 406–415, https://doi.org/10.1016/j.jmbbm.2018.12.033.
[43] S. Butylina, S. Geng, K. Oksman, Properties of as-prepared and freeze-dried hydrogels made from poly(vinyl alcohol) and cellulose nanocrystals using freeze-thaw technique, Eur. Polym. J. 81 (2016) 386–396, https://doi.org/10.1016/j.eurpolymj.2016.06.028.
[44] X.-Q. Hu, D.-Z. Ye, J.-B. Tang, L.-J. Zhang, X. Zhang, From waste to functional additives: thermal stabilization and toughening of PVA with lignin, RSC Adv. 6 (2016) 13797–13802, https://doi.org/10.1039/C5RA26385A.
[45] Y. Chen, K. Zheng, L. Niu, Y. Zhang, Y. Liu, C. Wang, F. Chu, Highly mechanical properties nanocomposite hydrogels with biorenewable lignin nanoparticles, Int. J. Biol. Macromol. 128 (2019) 414–420, https://doi.org/10.1016/j.ijbiomac.2019.01.099.
[46] A.B. Albadarin, M.N. Collins, M. Naushad, S. Shirazian, G. Walker, C. Mangwandi, Activated lignin-chitosan extruded blends for efficient adsorption of methylene blue, Chem. Eng. J. 307 (2017) 264–272, https://doi.org/10.1016/j.cej.2016.08.089.
[47] H. Qian, J. Wang, L. Yan, Synthesis of lignin-poly(N-methylaniline)-reduced graphene oxide hydrogel for organic dye and lead ions removal, J. Bioresour. Bioprod. 5 (2020) 204–210, https://doi.org/10.1016/j.jobab.2020.07.006.
[48] L. Wu, S. Huang, J. Zheng, Z. Qiu, X. Lin, Y. Qin, Synthesis and characterization of biomass lignin-based PVA super-absorbent hydrogel, Int. J. Biol. Macromol. 140 (2019) 538–545, https://doi.org/10.1016/j.ijbiomac.2019.08.142.
[49] Y. Meng, C. Li, X. Liu, J. Lu, Y. Cheng, L.-P. Xiao, H. Wang, Preparation of magnetic hydrogel microspheres of lignin derivate for application in water, Sci. Total Environ. (2019), https://doi.org/10.1016/j.scitotenv.2019.06.278.
[50] X.J. Liu, M.F. Li, S.K. Singh, Manganese-modified lignin biochar as adsorbent for removal of methylene blue, J. Mater. Res. Technol. 12 (2021) 1434–1445, https://doi.org/10.1016/j.jmrt.2021.03.076.
[51] R.A. Batista, P.J.P. Espitia, J.S.S. de Quintans, M.M. Freitas, M.Â. Cerqueira, J. A. Teixeira, J.C. Cardoso, Hydrogel as an alternative structure for food packaging systems, Carbohydr. Polym. 205 (2019) 106–116, https://doi.org/10.1016/j.carbpol.2018.10.006.
[52] N. Nguyen Van Long, C. Joly, P. Dantigny, Active packaging with antifungal activities, Int. J. Food Microbiol. 220 (2016) 73–90, https://doi.org/10.1016/j.ijfoodmicro.2016.01.001.
[53] O.Y. Abdelaziz, D.P. Brink, J. Prothmann, K. Ravi, M. Sun, J. García-Hidalgo, M. Sandahl, C.P. Hulteberg, C. Turner, G. Lidén, M.F. Gorwa-Grauslund, Biological valorization of low molecular weight lignin, Biotechnol. Adv. 34 (2016) 1318–1346, https://doi.org/10.1016/j.biotechadv.2016.10.001.
[54] R. Fernández-Marín, M. Mujtaba, D. Cansaran-Duman, G. Ben Salha, M.Á. A. Sánchez, J. Labidi, S.C.M. Fernandes, Effect of deterpenated origanum majorana l. Essential oil on the physicochemical and biological properties of chitosan/β-chitin nanofibers nanocomposite films, Polymers (Basel). 13 (2021), https://doi.org/10.3390/polym13091507.
[55] D. Dey, V. Dharini, S.P. Selvam, E.R. Sadiku, M.M. Kumar, J. Jayaramudu, U. N. Gupta, Physical, antifungal, and biodegradable properties of cellulose nanocrystals and chitosan nanoparticles for food packaging application, Mater. Today Proc. 38 (2021) 860–869, https://doi.org/10.1016/j.matpr.2020.04.885.
[56] I. Zarandona, A.I. Puertas, M.T. Dueñas, P. Guerrero, K. de la Caba, Assessment of active chitosan films incorporated with gallic acid, Food Hydrocoll. 101 (2020), https://doi.org/10.1016/j.foodhyd.2019.105486.